

Synthesis of Random Antenna Array Patterns with Prescribed Nulls

YEHESKEL BAR-NESS, SENIOR MEMBER, IEEE, AND ALEXANDER M. HAIMOVICH, MEMBER, IEEE

Abstract—Under study is a method devised to reduce sidelobes of thinned random antenna arrays over specified angular sectors. The thinned array is assumed random in the sense that the nominal location of the elements is known, but their actual position may vary randomly. It is shown that by imposing adequately dense pattern nulls, it is possible to reduce the sidelobes effectively in the region of the nulls. The problem is formulated as a set of points in the radiation pattern, which are constrained to specified values. The unknowns are the excitations, or weights, applied to the array elements. In the general case, the linear system of equations is consistent and has an infinite number of solutions. The solution selected optimizes the pattern in a minimum variance sense. Quantitative relations are derived for the pattern change and the gain cost associated with the imposed pattern nulls. Several examples are included to illustrate the results.

I. INTRODUCTION

THE RELATIONSHIP of directive gain to sidelobe level is an important measure in considerations related to the radiation pattern of an antenna. Regarding the output of the antenna as an image of several illuminated objects, the relation between main beam intensity and the average sidelobe intensity determines the contrast when the image is scanned. The peak sidelobe sets a limit to the dynamic range of the system. Because of the importance of these parameters, the synthesis of phased array patterns receives much attention. Control of the radiation pattern may be attained either by excitation or element spacing. Dolph [1] considered the required excitations at isotropic uniformly spaced elements to obtain a minimum main beamwidth for a specified sidelobe level. The result is known as a Dolph-Chebyshev array. This work was later extended by Baklanov [2] to the case of nonuniformly spaced elements with equal excitations. The performance of a linear phased thinned array when the spacing between adjacent elements is increased linearly or exponentially was studied by Hicks and Patel [3]. However, practical considerations limit the applicability of such systems to cases where accurate deployment of elements is possible. A long non-rigid array is an example where these methods are not very useful.

Large thinned arrays are of much interest for high resolution applications. A thinned array for which the element locations are chosen randomly and independently is called a random array. These arrays were first studied by Lo [4]. It turns out that the probability distribution function of the element location determines the shape of radiation pattern only in the neighborhood of the main beam. The pattern distant from the main lobe has a random nature that gives rise to high peak sidelobes.

Thinned periodic arrays were shown to offer very low side-

lobes but have the ambiguity problem represented by grating lobes [5]. For random arrays diversity methods were examined. Independent patterns are created by means of position or wavelength diversity, and then averaged [5]. The method has the shortcoming of practical difficulty in creating the independent patterns. The present work attempts to reduce sidelobes of a thinned random array in certain directions by imposing nulls in the radiation pattern. A similar method was considered recently by Steyskal [6] for the periodic nonrandom array. A set of nominal element locations is assumed known. The nonrigidity of the array begets random differences between the actual and nominal positions. It is in this sense that the array is assumed random. The statistics of the array pattern contain information about the sidelobe characteristics. The method described in the following sections alters the statistics of the random array in a way that is shown to improve sidelobe characteristics.

II. FORMULATION OF THE PROBLEM

Consider a linear array with N isotropic antennas distributed over an aperture of length L . Let x_1, x_2, \dots, x_N be the locations of the array elements with respect to an origin arbitrarily picked at the midpoint of the aperture. A complex weight or excitation w_n is associated with each element x_n . The angle θ is measured with respect to the normal to the array and $u = \sin \theta$. The first case to be considered is the far-field pattern. The array factor is

$$f(u) = \sum_{n=1}^N w_n^* e^{jkx_n u} \quad (1)$$

where the asterisk denotes the complex conjugate, $k = 2\pi/\lambda$ is the wavenumber, and λ is the wavelength. In a random array, the element positions are chosen from a set of independent random variables with given probability distribution function. Since the locations x_n are random numbers, $f(u)$ is a random process. The expectation of $f(u)$ is the average array factor and can be matched to any desired pattern by selecting an appropriate probability distribution function (pdf) of the element locations [7]. The expectation of $|f(u)|^2$ is the power pattern. The variance of $f(u)$ is a measure of the spread of the pattern around a prescribed average. We list the following objectives.

- 1) Determine the complex weights to be applied to the array elements such that in prescribed directions the average array factor is nulled, and the variance of array factor is minimized. The main beam is to be preserved in the desired direction.
- 2) Determine the relation between the statistics of the element locations and the variance of the array factor.
- 3) Determine the directions of the forced nulls so as to synthesize a pattern that contains a reduced sidelobe in a prescribed wide-angle sector.

Manuscript received February 27, 1984; revised June 29, 1984.

Y. Bar-Ness was with Drexel University, Philadelphia, PA. He is now with Bell Laboratories, Holmdel, NJ 07733.

A. Haimovich was with Drexel University, Philadelphia, PA. He is now with AEL, Inc., P. O. Box 552, Lansdale, PA 19446.

III. METHOD OF SOLUTION

Pursuing the above objectives, we consider weight vector $\mathbf{W}^T = (w_1, \dots, w_N)$ solutions to the following set of equations:

$$\begin{aligned} E\{w_1^* e^{jkx_1 u_0} + \dots + w_N^* e^{jkx_N u_0}\} &= \alpha N \\ E\{w_1^* e^{jkx_1 u_1} + \dots + w_N^* e^{jkx_N u_1}\} &= 0 \\ &\vdots \\ E\{w_1^* e^{jkx_1 u_M} + \dots + w_N^* e^{jkx_N u_M}\} &= 0 \end{aligned} \tag{2}$$

where the expectation is taken with respect to the pdf of the element locations. The first equation in the system represents the main beam with direction $u_0 = \sin \theta_0$. In a nonconstrained random array, w_n^* are chosen as conjugates of $e^{jkx_n u_0}$ and yield $f(u_0) = N$. In the constrained array (2), $\alpha < 1$ represents a main lobe degradation that is allowed by the design. It arises from the assignment of M degrees of freedom to nulling. The remaining M equations in (2) state that w_n are to be chosen so as to equate the average array factor $E\{f(u)\}$ to zero in the specified directions u_1, u_2, \dots, u_M . Observe that any solution of (2) will null the average array factor in these directions as required by objective 1).

For $M + 1 < N$, (2) is a consistent linear system of equations and has an infinite number of solutions. From all possible solutions, the one that yields the minimum variance of the array factor is selected as follows. To each element in the array, (2) associates an expression $E\{w_n^* e^{jkx_n u}\} = w_n^* E\{e^{jkx_n u}\}$. Letting the nominal location of the n th element be a_n ; the pdf of the actual location x_n is $p(x_n - a_n)$. Then

$$E\{e^{jkx_n u}\} = \int_{-\infty}^{\infty} p(x_n - a_n) e^{jkx_n u} dx_n. \tag{3}$$

Changing variables, $y_n = x_n - a_n$, we have

$$\begin{aligned} E\{e^{jkx_n u}\} &= e^{jka_n u} \int_{-\infty}^{\infty} p(y_n) e^{jky_n u} dy_n \\ &= \eta(u) e^{jka_n u} \end{aligned} \tag{4}$$

where $\eta(u)$ is the inverse Fourier transform of $p(y_n)$ and is a function of the angle variable u . Defining the array matrix R , where $(R)_{nm} \triangleq E\{e^{jkx_n u_m}\} = \eta(u_m) e^{jka_n u_m}$, and the constraint vector

$$\mathbf{c}^T \triangleq (\alpha N, 0, \dots, 0), \tag{5}$$

then system (2) becomes

$$R' \mathbf{W} = \mathbf{c} \tag{6}$$

where the prime denotes complex conjugate and transpose.

Next we compute the average power pattern:

$$\begin{aligned} E\{|f(u)|^2\} &= E\{\mathbf{W}' \mathbf{x}(u) \mathbf{x}'(u) \mathbf{W}\} \\ &= \mathbf{W}' E\{\mathbf{x}(u) \mathbf{x}'(u)\} \mathbf{W} \end{aligned}$$

where

$$\mathbf{x}^T(u) \triangleq \{e^{jkx_1 u}, \dots, e^{jkx_N u}\}, \tag{7}$$

and

$$E\{\mathbf{x}(u) \mathbf{x}'(u)\} = \begin{bmatrix} 1 & E\{e^{jk(x_1 - x_2)u}\} & E\{e^{jk(x_1 - x_N)u}\} \\ \vdots & \vdots & \vdots \\ E\{e^{-jk(x_1 - x_N)u}\} & E\{e^{-jk(x_2 - x_N)u}\} & \dots & 1 \end{bmatrix}$$

Because x_i and x_j are independent random variables for all $i \neq j$, using (4) yields

$$\begin{aligned} E\{e^{jk(x_i - x_j)u}\} &= E\{e^{jkx_i u}\} E\{e^{-jkx_j u}\} \\ &= \eta^2(u) e^{jk(a_i - a_j)u}. \end{aligned} \tag{8}$$

Using this result, we have for the average power

$$E\{|f(u)|^2\} = (1 - \eta^2(u)) \mathbf{W}' \mathbf{W} + \eta^2(u) |\mathbf{W}' \mathbf{A}(u)|^2 \tag{9}$$

where

$$\mathbf{A}^T(u) \triangleq \{e^{jka_1 u}, \dots, e^{jka_n u}\}. \tag{10}$$

The variance of the array factor normalized to the main beam power $(\alpha N)^2$ is

$$\begin{aligned} \sigma^2(u) &= \frac{1}{(\alpha N)^2} [E\{|f(u)|^2\} - E\{f(u)\} E\{f^*(u)\}] \\ &\quad - \frac{1}{(\alpha N)^2} [(1 - \eta^2(u)) \mathbf{W}' \mathbf{W} + \eta^2(u) |\mathbf{W}' \mathbf{A}(u)|^2 \\ &\quad - \eta^2(u) |\mathbf{W}' \mathbf{A}(u)|^2] \\ \sigma^2(u) &= \frac{1}{(\alpha N)^2} (1 - \eta^2(u)) \|\mathbf{W}\|^2. \end{aligned} \tag{11}$$

Equation (11) holds for any direction u .

The solution of (2) that minimizes (11) is the weight vector \mathbf{W} that has minimum norm $\|\mathbf{W}\|^2$. Since a consistent linear system has a unique solution with minimum norm [8], we have

$$\mathbf{W} = R^+ \mathbf{c} \tag{12}$$

where R^+ is the generalized inverse of R , defined as $R^+ = R(R'R)^{-1}$. In the Appendix we evaluate the relationship between the weight vector with minimum norm and the main lobe degradation factor α ; viz,

$$\|\mathbf{W}\|^2 = \frac{\alpha^2 N^2}{\eta^2(u_0)(N - M)} \tag{13}$$

where u_0 is the direction of the main lobe.

Notice that for the nonconstrained random array, $\|\mathbf{W}\|^2 = N$. To be able to compare the two arrays we use for the constraint array $\|\mathbf{W}\|^2 = N$, which can be obtained by adjusting the weight gain. With this the degradation factor of the main lobe due to the constraints becomes

$$\alpha^2 = \frac{\eta^2(u_0)(N - M)}{N}. \tag{14}$$

Using (13) in (11) the variance of the array factor becomes

$$\sigma^2(u) = \frac{1 - \eta^2(u)}{\eta^2(u_0)(N - M)}. \tag{15}$$

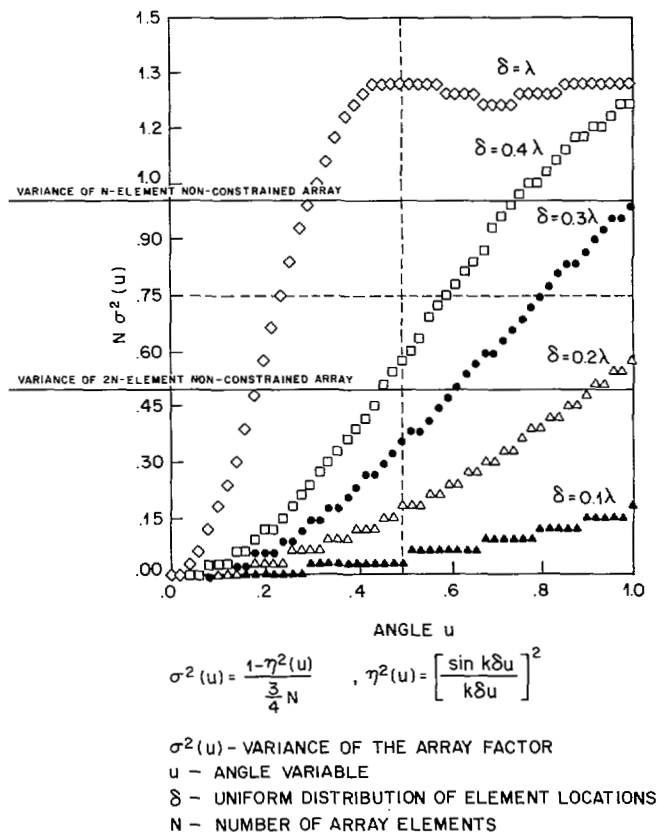


Fig. 1. Variance of array factor.

Fig. 1 depicts $\sigma^2(u)$ for a case where $M = (1/4)N$ and the pdf of element locations is uniform, i.e.;

$$p(x_n - a_n) = \begin{cases} 1/2\delta, & -\delta \leq x_n - a_n \leq \delta \\ 0, & \text{otherwise.} \end{cases} \quad (16)$$

Hence, $\eta^2(u) = (\sin k\delta u / k\delta u)^2$. The main lobe is steered to broadside so that $u_0 = 0$ and $\eta^2(u_0) = 1$. Recalling that the variance of a N -element nonconstrained array factor is $1/N$ [7], we observe that the N -element constrained array features a variance comparable with a $2N$ -element nonconstrained array, when $\delta = 0.2\lambda$. That is with the method proposed there is a possible savings of half the number of elements while maintaining the same variance, and thus the same sidelobes. Obviously when there is no uncertainty in element locations ($\delta = 0$) the pattern is a deterministic function and $\sigma^2 = 0$. While the reduction in the variance occurs at all angles it is only at u_m , $m = 1, \dots, M$, where, as indicated by (2), the average array factor $E\{f(u_m)\} = 0$. From comparing (9) and (11) we notice that in these directions, the normalized power pattern $1/(\alpha N)^2 E\{|f(u)|^2\}$ coincides with the variance of the array factor $\sigma^2(u)$. That is

$$\sigma^2(u_m) = \frac{1}{(\alpha N)^2} E\{|f(u_m)|^2\}, \quad m = 1, \dots, M. \quad (17)$$

Having considered objectives (1) and (2) we next turn to the question of how the radiation pattern is interpolated at points between the forced nulls and where the nulls should be placed in order to synthesize a pattern with reduced sidelobes in a prescribed sector.

IV. SIDELOBE REDUCTION OVER SECTORS

The objective is to control the array pattern over an angular sector rather than in prescribed directions. Intuitively it is perceived that if the nulls are placed densely enough, sidelobes in the nulls' vicinity will be reduced. One possible approach is to make use of the sampling theorem. Following the argument in [9] for an array aperture of L , (1) is the Fourier series representation of $f(u)$ and the numbers x_n may be considered the frequency components of $f(u)$. Since all $|x_n| \leq L/2$, $f(u)$ is band-limited to $|x| < L/2$. According to the sampling theorem $f(u)$ is completely specified by its values $1/L$ apart, and the power pattern $|f(u)|^2$ by values $1/2L$ apart. Let $P(u) \triangleq 1/(\alpha N)^2 E\{|f(u)|^2\}$, then,

$$P(u) = \sum_{j=-\infty}^{\infty} P(j/2L) \frac{\sin 2\pi L(u - j/2L)}{2\pi L(u - j/2L)}. \quad (18)$$

It is observed that $P(u)$ is mostly affected by values $P(j/2L)$ at $j/2L$ close to u . As $u - j/2L$ increases so diminishes the contribution of the respective $P(j/2L)$ to $P(u)$. To further elaborate on the point we write the following, which is equivalent to (18) and which employs differences of the sampled values [10].

$$\begin{aligned} P\left(u_m + \xi \frac{1}{2L}\right) &= P(u_m) + \xi \left[P\left(u_m + \frac{1}{2L}\right) - P(u_m) \right] \\ &+ \frac{1}{2!} \xi(\xi - 1) \left[P\left(u_m + \frac{1}{2L}\right) - 2P(u_m) \right. \\ &\left. + P\left(u_m - \frac{1}{2L}\right) \right] + \dots \end{aligned} \quad (19)$$

where $|\xi| \leq 1$.

An estimate of the error when using n terms is found in [11].

$$R_n\left(u_m + \frac{1}{2L}\right) \cong \frac{\pi_n(\xi)}{(n+1)!} \Delta^{n+1} P(u_m) \quad (20)$$

where $\pi_n(\xi)$ is a polynomial in ξ of degree $n+1$ and Δ^{n+1} is the $n+1$ th order difference of $P(u_m)$. The values of $P(u_m) = 1/(\alpha N)^2 E\{|f(u_m)|^2\} = \sigma^2(u_m)$ are determined by (15). $\sigma(u_m)$ being a smooth function, as shown in Fig. 1, $P(u_m + \xi(1/2L))$ will be determined by a few difference terms around u_m . Reducing $\sigma^2(u)$ at $u = u_m$ will reduce $P(u_m + \xi(1/2L))$. Now consider the sector interval limited by nulls at u_1 and u_m , with the other nulls being prescribed at $u_m = u_1 + (m-1)/2L$. It is expected to obtain an array pattern with lower sidelobes over the entire interval, except the sector margins. Examples of Section VIII supports this assertion. A case with nulls more sparsely spaced ($1/L$ instead of $1/2L$ in Fig. 11) is also examined, indicating higher sidelobes but still showing overall reduction compared with a nonconstrained array.

V. EFFECT OF CONSTRAINED NULLS ON THE PATTERN

Forcing the pattern to have nulls in certain directions is expected to affect the pattern over the entire angular sector. The unconstrained complex pattern, in which the weight vector is

taken to steer the main beam at $u_0 = 0$, is $E\{P(u)\} = \mathbf{1}^T \mathbf{A}(u)$ where $\mathbf{1}^T = (1, \dots, 1)$ is an N -dimension weight vector, and $\mathbf{A}(u)$ is defined in (10). The constrained complex pattern is $E\{f(u)\} = \mathbf{W}' \mathbf{A}(u)$. The difference between the two patterns is

$$D(u) = (\mathbf{1}^T - \mathbf{W}'^T) \mathbf{A}(u).$$

An overall measure of the difference between the two patterns is defined as

$$F = \frac{1}{N^2} \int_{-1}^{+1} |D(u)|^2 du. \tag{21}$$

It is possible to find an upper bound on F

$$\begin{aligned} F &= \frac{1}{N^2} \int_{-1}^1 |D(u)|^2 du = \frac{1}{N^2} \int_{-1}^1 |(\mathbf{1}^T - \mathbf{W}'^T) \mathbf{A}(u)|^2 du \\ &\leq \frac{2}{N^2} \|\mathbf{1}^T - \mathbf{W}'^T\|^2 \int_{-1}^1 |\mathbf{A}(u)|^2 du. \end{aligned} \tag{22}$$

But

$$\|\mathbf{1}^T - \mathbf{W}'^T\|^2 = \|\mathbf{1}\|^2 + \|\mathbf{W}'\|^2 - 2 \operatorname{Re}\{\mathbf{1}^T \mathbf{W}'\} \tag{23}$$

where $\|\mathbf{1}\|^2 = N$, $\|\mathbf{W}'\|^2 = N$ and $\mathbf{1}^T \mathbf{W}' = \alpha N$ (first equation in system (2) with $u_0 = 0$) (23) becomes

$$\|\mathbf{1}^T - \mathbf{W}'^T\|^2 = 2N(1 - \alpha). \tag{24}$$

Also

$$|\mathbf{A}(u)|^2 = \sum_{n=1}^N |e^{jka_n u}|^2 = N. \tag{25}$$

Substituting (24), (25) in (22)

$$F \leq 4(1 - \alpha). \tag{26}$$

The last result indicates that the change in the radiation pattern caused by imposing nulls depends on α , a factor which relates the number of constraints to the number of elements in the array. For a given number of elements, changes in pattern grow in significance with the number of constraints.

VI. NEAR FIELD

Following the method of solution for the far field we rewrite system (2) for the near-field case.

$$\begin{aligned} E\{\mathbf{W}' \mathbf{x}(u_0, \rho)\} &= \alpha N \\ E\{\mathbf{W}' \mathbf{x}(u_1, \rho)\} &= 0 \\ &\vdots \\ E\{\mathbf{W}' \mathbf{x}(u_M, \rho)\} &= 0 \end{aligned} \tag{27}$$

where ρ is the focal distance and \mathbf{x} is defined by

$$\begin{aligned} \mathbf{x}^T(u, \rho) &= \left\{ \exp \left[jk \left(x_1 u - \frac{x_1^2}{2\rho} \right) \right], \dots, \right. \\ &\quad \left. \exp \left[jk \left(x_N u - \frac{x_N^2}{2\rho} \right) \right] \right\}. \end{aligned}$$

For all possible solutions of (27) we again choose the one which yields an array factor with minimum variance. For this case:

$$\begin{aligned} E \left\{ \exp \left[jk \left(x_n u - \frac{x_n^2}{2\rho} \right) \right] \right\} \\ = \int_{-\infty}^{\infty} p(x_n - a_n) \exp \left[jk \left(x_n u - \frac{x_n^2}{2\rho} \right) \right] dx_n. \end{aligned}$$

Changing variables, $y_n = x_n - a_n$, the right side of this equation becomes

$$\begin{aligned} &= \exp \left[jk \left(a_n u - \frac{a_n^2}{2\rho} \right) \right] \int_{-\infty}^{\infty} p(y_n) \\ &\quad \cdot \exp \left[jky_n \left(u - \frac{a_n}{\rho} \right) \right] \exp \left[-jk \frac{y_n^2}{2\rho} \right] dy_n. \end{aligned} \tag{28}$$

To further develop the last expression we use the far-field condition, viz,

$$\frac{L^2}{\lambda \rho} \ll 1 \tag{29}$$

where L is the array aperture. With y_n , the uncertainty in the location of the n th element, of the order of λ , and L many times greater than λ , it is clear that

$$\frac{ky_n^2}{2\rho} = \frac{2\pi}{\lambda} \frac{y_n}{\rho} \frac{y_n}{\rho} < \frac{L}{\rho} < \frac{L^2}{\lambda \rho} \ll 1.$$

Therefore $\exp[-jk(y_n^2/2\rho)] \cong 1$ and (28) becomes

$$\begin{aligned} E \left\{ \exp \left[jk \left(x_n u - \frac{x_n^2}{2\rho} \right) \right] \right\} \\ = \eta \left(u - \frac{a_n}{\rho} \right) \exp \left[jk \left(a_n u - \frac{a_n^2}{2\rho} \right) \right] \end{aligned} \tag{30}$$

where

$$\eta \left(u - \frac{a_n}{\rho} \right) = \int_{-\infty}^{\infty} p(y_n) \exp \left[jky_n \left(u - \frac{a_n}{\rho} \right) \right] dy_n.$$

Since $a_n/\rho \ll 1$ then for pdf's that are of interest, e.g., uniform, Gaussian, and u small enough, $\eta(u - a_n/\rho) \cong \eta(u)$ (see example in Fig. 2). Hence except for the quadrature phase term, the analysis done for the far field is in effect for the near-field case. In particular, in order to minimize the variance of the array factor in the near field we must find the minimum norm vector \mathbf{W} ,

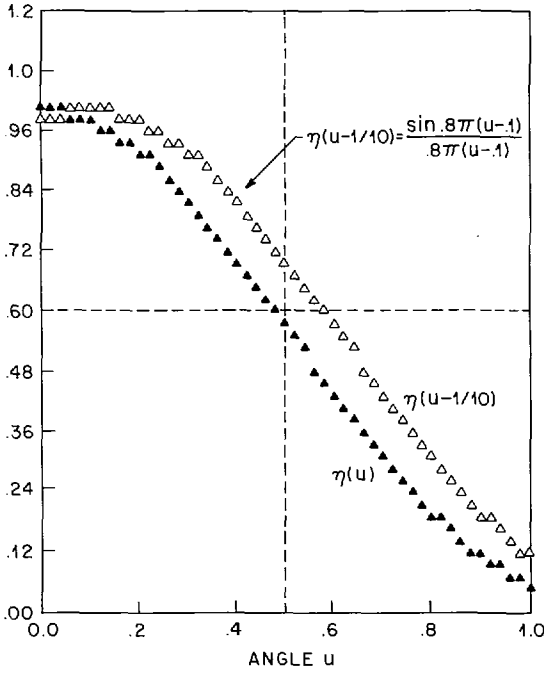
$$\mathbf{W} = \mathbf{Q}^+ \mathbf{c}$$

where $\mathbf{Q}^+ = \mathbf{Q}(\mathbf{Q}'\mathbf{Q})^{-1}$, \mathbf{c} is the constraint vector defined by (5) and

$$(\mathbf{Q})_{nm} = \eta(u_m) \exp [jk(a_n u_m - a_n^2/\rho)].$$

VII. BANDWIDTH CONSIDERATIONS

As long as the received signal is narrowband it can be adequately characterized by a single frequency ω_c . The relation between radiation pattern and wavelength is emphasized when



$$\eta(u) = \frac{\sin k \delta u}{k \delta u}$$

WITH $k = \frac{2\pi}{\lambda}$, $\delta = 0.4\lambda$ $\eta(u) = \frac{\sin .8\pi u}{.8\pi u}$

$$\eta(u - a_n/\rho) = \frac{\sin k \delta (u - a_n/\rho)}{k \delta (u - a_n/\rho)}$$

WITH $a_n/\rho = 1/10$ $\eta(u - 1/10) = \frac{\sin .8\pi (u - 1/10)}{.8\pi (u - 1/10)}$

Fig. 2. Approximation of $\eta(u)$.

(1) is rewritten as

$$f(u) = \sum_{n=1}^N w_n^* \exp\left(j \frac{\omega}{c} x_n u\right) \quad (31)$$

where c is the speed of light. The array vector that includes dependence on frequency is

$$\mathbf{x}^T(u, \omega_1) = \left\{ \exp\left(j \frac{\omega_1}{c} x_1 u\right), \dots, \exp\left(j \frac{\omega_1}{c} x_N u\right) \right\}. \quad (32)$$

The array factor will be

$$f(u) = \mathbf{W}' \int S(\omega_1 - \omega_0) \mathbf{x}(u, \omega_1) d\omega_1$$

where $S(\omega)$ is the base-band equivalent of signal spectrum and ω_0 is the middle frequency.

The problem can therefore be formulated in terms of the expectation of the array factor with respect to the pdf of the element locations, viz,

$$E\{f(u)\} = E\left\{ \mathbf{W}' \int S(\omega_1 - \omega_0) \mathbf{x}(u, \omega_1) d\omega_1 \right\}.$$

For each component of $\mathbf{x}(u, \omega_1)$

$$E\left\{ \exp\left(j \frac{\omega_1}{c} x_n u\right) \right\} = \iint S(\omega_1 - \omega_0) p(x_n - a_n) \cdot e^{j(\omega_1/c)x_n u} dx_n d\omega_1.$$

Changing variables $y_n = x_n - a_n$, $\omega = \omega_1 - \omega_0$ and noting that all elements have the same pdf $p(y_n) = p(y)$,

$$\begin{aligned} E\left\{ \exp\left(j \frac{\omega_1}{c} x_n u\right) \right\} \\ &= e^{j(\omega_0/c)a_n u} \int S(\omega) e^{j(\omega a_n u/c)} \int p(y) e^{j(\omega + \omega_0/c)y u} dy d\omega \\ &= e^{j(\omega_0/c)a_n u} \int S(\omega) \eta\left(\frac{\omega + \omega_0}{c} u\right) e^{j(\omega a_n u/c)} d\omega. \end{aligned} \quad (34)$$

For small signal bandwidth the argument of η changes only slightly so that the right side of (34) can be approximated by

$$\begin{aligned} &= e^{j(\omega_0/c)a_n u} \eta\left(\frac{\omega_0}{c} u\right) \int S(\omega) e^{j(\omega a_n u/c)} d\omega \\ &= s\left(\frac{a_n u}{c}\right) \eta\left(\frac{\omega_0}{c} u\right) e^{j(\omega_0 a_n/c)u} \end{aligned} \quad (35)$$

where $s(t)$ is the inverse Fourier transform of $S(\omega)$. In order to be able to use the method of Section III for the nonzero bandwidth case, $s(a_n u/c)$ needs to be almost constant over a_n within the array aperture, i.e., $|a_n| < L$. Since $c/a_n u \geq c/L$ for any u and a_n , therefore this condition is equivalent to require that the signal bandwidth be of the order of c/L . As an example, for 1000 λ array aperture and $\lambda = 3$ cm, the frequency content of the signal needs to be of the order of $c/L = 10$ MHz. Thus the proposed method can be applied only to narrow-band signals. This result is hardly surprising since the nulls are created by coherent contributions calculated at a given frequency. A change in frequency brings about changes in phase and loss of coherence.

VIII. EXAMPLES

In the following examples the array length is 100 λ . The nominal element locations were chosen independently from a set of uniformly distributed random numbers between -50 and 50 . The actual locations were displaced within a given tolerance. For example, for a tolerance $\delta = 0.2 \lambda$, a pattern is realized by adding to each location a displacement chosen from a uniform distribution between -0.1λ and 0.1λ . This realization is called a sample pattern. When radiation patterns of several samples are averaged, the result is called an average pattern. In the following examples average patterns were created out of ten samples. Patterns were created by interpolating values calculated at points $\lambda/2L$ apart. The number of imposed nulls in a pattern was $M = 6$. The ordinate scale is in dB and the abscissa is linear in the angular variable $u = \sin \theta$. Values are normalized to N^2 , which is the power of the main beam of a N -element unconstrained random array.

The first group of patterns deals with a 20-element array. Fig. 3 shows the pattern of the unconstrained array. The weight vector is set to steer the main beam to broadside ($u_0 = 0$). The pattern is symmetrical, and it exhibits random characteristics except in the immediate vicinity of the main beam. High peak sidelobes of up to -6 dB below the main beam are visible. The constrained pattern is created by letting the angle variable $u_m = 0.36 + 0.005(m - 1)$, $m = 1, \dots, 5$, where $0.005 = 1/2L = 1/200$. Then to find the weight vector \mathbf{W} system (2) is solved by (12). The levels obtained at these null locations are limited by

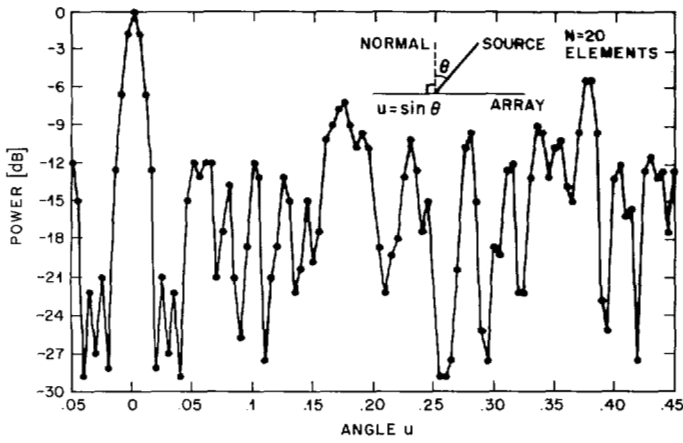


Fig. 3. Radiation pattern, unconstrained.

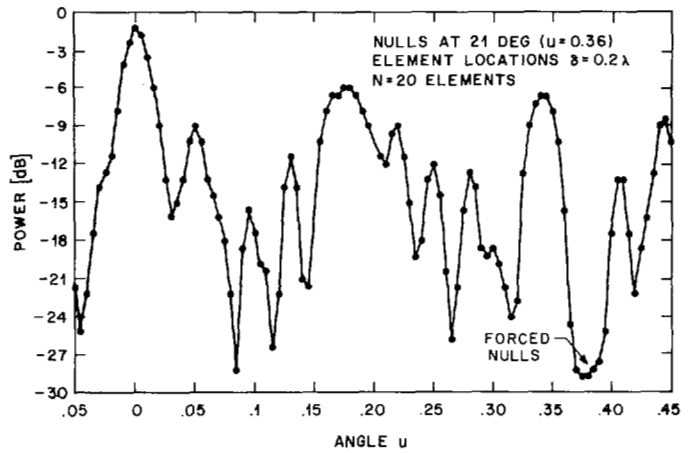


Fig. 5. Radiation pattern, average, $\delta = 0.2$

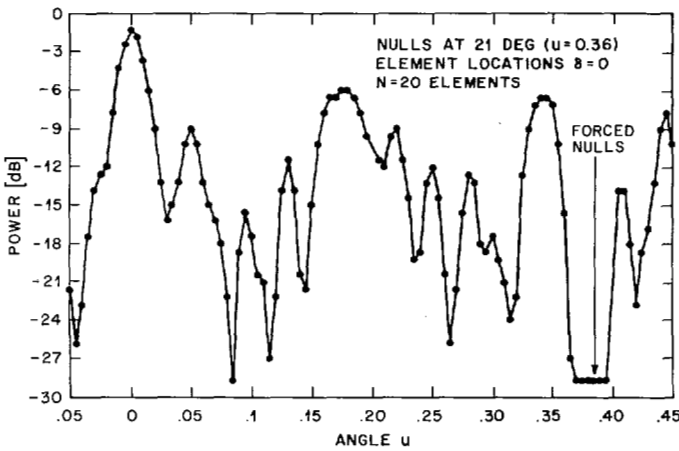


Fig. 4. Radiation pattern, constrained, $\delta = 0$.

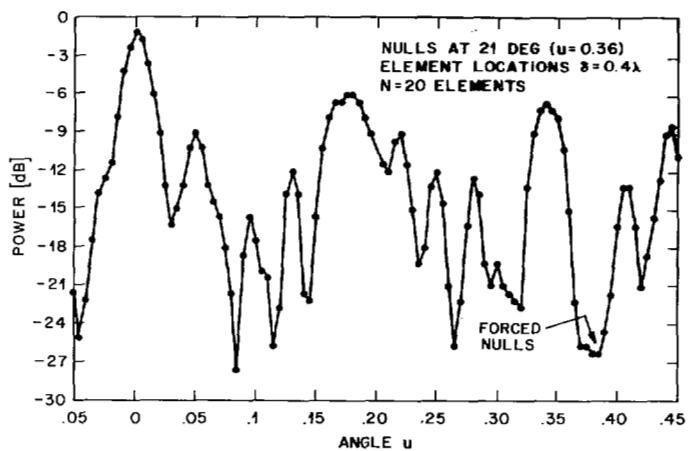


Fig. 6. Radiation pattern, average, $\delta = 0.4$.

the plot at -29 dB. Fig. 4 shows the constrained array pattern with $\delta = 0$.¹ The five nulls appear as anticipated at the prescribed locations. Moreover these nulls pull down the sidelobes in their vicinity. The nulls were purposely imposed at locations where a high peak sidelobe in the unconstrained array of Fig. 3 occurs. A sidelobe appears in Fig. 4, slightly translated by the nulls, from the position of the sidelobe in the unconstrained array. The main beam is reduced by -1.2 dB as anticipated by (14); viz,

$$10 \log \alpha^2 = 10 \log (\eta^2(u_0)(N - M)/N) = 10 \log (15/20) = -1.2 \text{ dB.}$$

The noted symmetry of the unconstrained pattern disappears in this constrained array pattern which looks quite different from the unconstrained pattern. The last point will be further elaborated on later in this section.

Figs. 5, 6, and 7 represent average patterns made of ten independent samples with tolerances on element locations of $\delta = 0.2 \lambda$, 0.4λ , and 1.0λ , respectively. The randomization of the element locations introduces values different from zero at the prescribed points. Nevertheless, comparing Fig. 3, which is a particular realization of a nonconstrained array, with Figs. 5,

¹ $\delta = 0$, means that the constrained array element locations (Fig. 4) are the same as those locations chosen for the unconstrained random array of Fig. 3. Notice that these latter locations were chosen randomly in the interval $(-L/2, L/2)$.

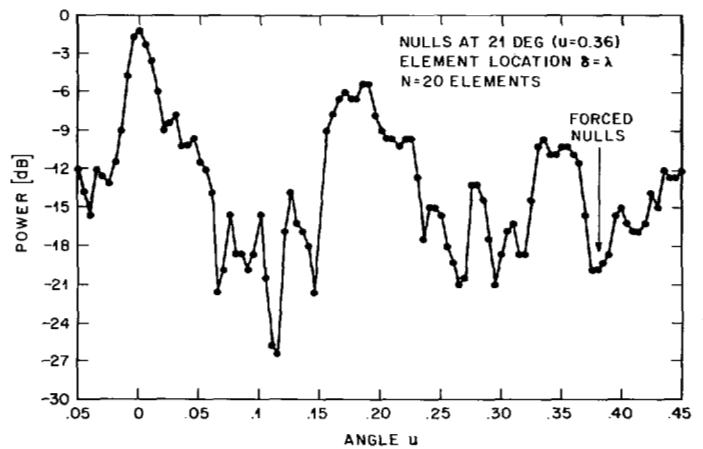


Fig. 7. Radiation pattern, average, $\delta = \lambda$.

6, and 7 we observe that the sidelobes are reduced in the region where the nulls were imposed. It is expected that the sidelobes will be lower when the tolerance in element location is lower. Using Fig. 1 with $u = 0.38$ (mid-point of the nulls) the sidelobes for $\delta = 0.2 \lambda$ are expected to be lower by about 5.5 dB ($.075/.25$) than for $\delta = 0.4 \lambda$, and by about 10 dB ($.075/.90$) than for $\delta = 1.0 \lambda$. By comparing Figs. 5 and 6 we observe a 4 dB difference in the sidelobes at $u = 0.38$, Figs. 5 and 7 reveal a 9 dB difference. An interesting observation of a different

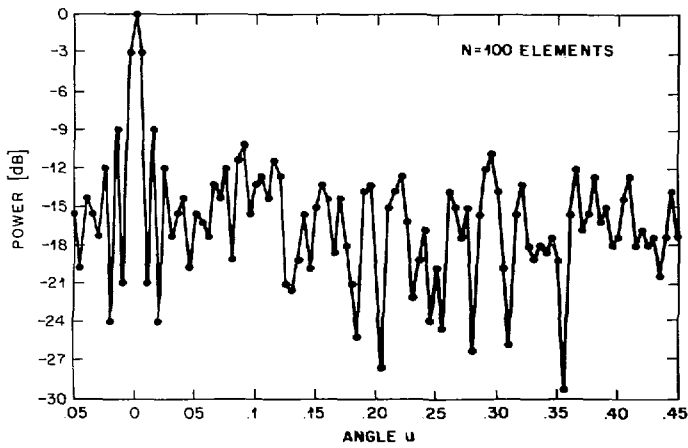


Fig. 8. Radiation pattern, unconstrained, 100 elements.

nature can be obtained by comparing Figs. 5 and 7. The pattern of Fig. 7 tends to be "smoother" than that in Fig. 5. This is because, with tolerance being $\delta = 0.2\lambda$, the patterns are summed almost coherently, while if $\delta = 1.0\lambda$, the patterns are independent, and therefore summed less coherently, resembling an integration or smoothing process.

We have shown by several examples that simulated patterns follow closely the predictions of the theory of Section III. Imposing nulls in the statistical sense of (2) actually reduces the side lobes for tolerances $\delta \leq \lambda$. When the tolerance is higher than λ and the actual and nominal element position can differ by one wavelength or more, the design and the actual pattern are uncorrelated, and the coherence needed to control the nulls efficiently is lost.

An unconstrained array with $N = 100$ elements, but with the same length $L = 100\lambda$ as in the previous example, is illustrated in Fig. 8. As in the case of the unconstrained array with 20 elements (Fig. 3), the pattern takes on random characteristics beyond approximately the third lobe. However, in the vicinity of the main lobe, a $(\sin x)/x$ type pattern is much more evident than in the case of 20 elements. Lower average sidelobes and peak sidelobes, as predicted by random array theory, are noticeable. Placing the five nulls in the region of relatively high sidelobes, at $u = 0.1$ and taking the tolerance to be $\delta = 0$, the resultant array pattern is depicted in Fig. 9. No reduction in the main lobe is observed as $\alpha^2 = -0.2$ dB is less than the resolution of the plot. Thus, in general terms this example follows the previous ones.

Next, we examine more closely the interpolated values between the prescribed nulls. This subject was referred to in Section IV. To this end, Fig. 10 magnifies the region of the constrained nulls of Fig. 4. Points between the imposed nulls are forced below -60 dB to -70 dB (Fig. 4 shows only -29 dB). These observations confirm the results of Section IV, which assert that if the nulls are sufficiently dense (at Nyquist interval $1/2L$), a sectoral sidelobe reduction will result. Furthermore, a Nyquist interval distance between the nulls is a sufficient but not necessary condition. Fig. 11 illustrates an array with 20 elements when the nulls are placed at intervals $1/L$ (rather than $1/2L$). The sidelobes are still reduced; however, the reduction is not substantial but is in trade-off with a sector twice as large.

The effects of null constraints on the radiation pattern were studied in Section V. To examine a concrete example Fig. 12 represents the ratio pattern (difference in dB) of the uncon-

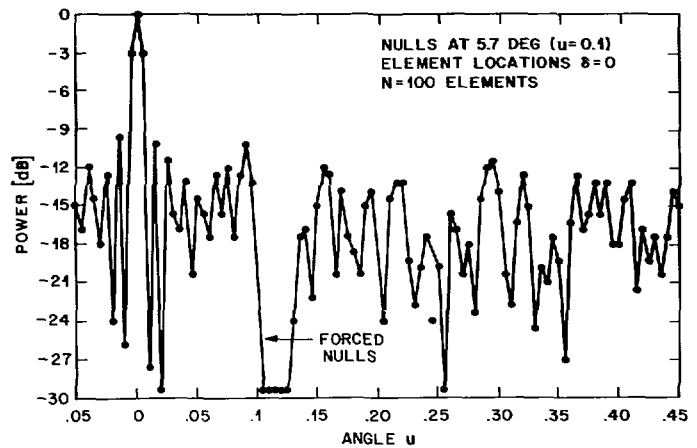


Fig. 9. Radiation pattern, constrained, 100 elements.

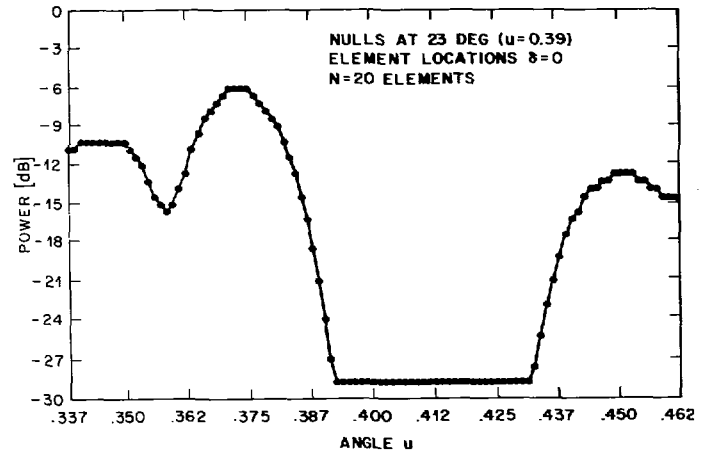


Fig. 10. Wide sector sidelobe reduction.

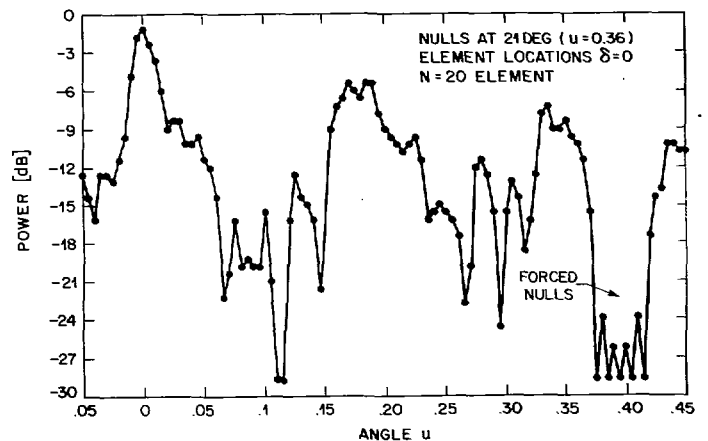


Fig. 11. Radiation pattern, distance between nulls $1/L$ $\delta = 0$.

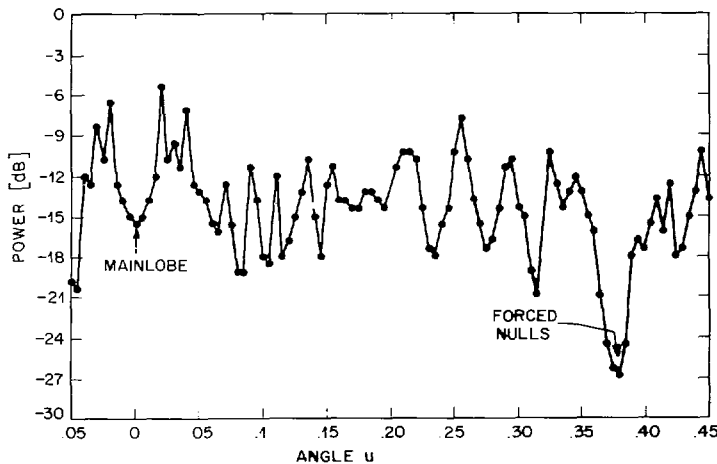


Fig. 12. Ratio of nonconstrained and constrained array patterns, 20 elements.

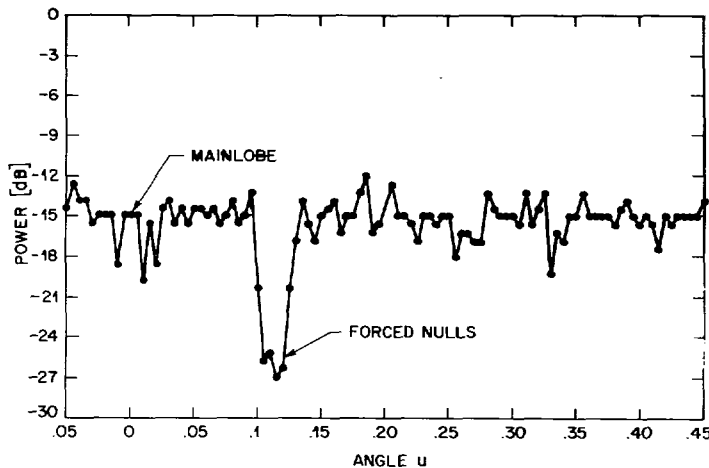


Fig. 13. Ratio of nonconstrained and constrained array patterns, 100 elements.

strained array of Fig. 3 and the constrained array with $\delta = 0$ of Fig. 4. Notice the large difference at $u = 0.36$ associated with the constrained nulls. The fluctuation in the ratio pattern indicates a significant change in the pattern.

Section V relates the change in the pattern to the factor α (26). Thus, for the same number of constraints and a larger number of elements $\alpha^2(=1 - M/N)$ (11) is increased and changes in the pattern should be less noticeable. This is illustrated in Fig. 13 which displays the ratio pattern (difference in dB) for the case of $N = 100$. Except for the large difference at the sector created by the forced nulls, the pattern is scarcely affected by the forced nulls.

IX. CONCLUSION

A method for synthesizing random antenna array patterns with prescribed nulls and with patterns being controlled by the array weights is proposed in this paper. The following conclusions were reached.

- 1) It is possible to have good control over prescribed nulls in the radiation pattern when the element locations are known with a tolerance of about one wavelength or better. The smaller the tolerance, the smaller the variance of the array pattern in the directions where nulls are imposed.
- 2) Setting the null constraints at intervals determined by the sampling theorem is sufficient for significant sidelobe reduction over wide sectors.
- 3) Diverting part of the degrees of freedom from beam cohering to nulling results in reduction of the main beam level. This main beam loss is proportional to the number of degrees of freedom used for nulling, relative to the total number of array elements.
- 4) The aforementioned conclusions can be extended to near-field radiation patterns.

APPENDIX

DERIVATION OF (13)

The objective of this Appendix is to evaluate the norm of the weight vector $\|W\|^2$. Using (12) and the definition of a generalized inverse yields

$$\|W\|^2 = W'W = c'[(R'R)^{-1}](R'R)(R'R)^{-1}c$$

$R'R$ is symmetric and therefore

$$\|W\|^2 = c'(R'R)^{-1}c \tag{36}$$

Now, $c^T = (\alpha N, 0, \dots, 0)$, hence

$$\|W\|^2 = \alpha^2 N^2 (R'R)^{-1}_{11} \tag{37}$$

where $(R'R)^{-1}_{11}$ is the (1, 1) element of $(R'R)^{-1}$.

Let $r^T(u) \triangleq \eta(u)(e^{jka_1u}, e^{jka_2u}, \dots, e^{jka_Nu})$ then

$$R'R = \begin{matrix} & \begin{matrix} B_{11} & & & B_{12} \end{matrix} \\ \begin{matrix} r'(u_0)r(u_0) & r'(u_0)r(u_1) & \cdots & r'(u_0)r(u_M) \\ \cdots & \cdots & \cdots & \cdots \\ r'(u_1)r(u_0) & r'(u_1)r(u_1) & \cdots & r'(u_1)r(u_M) \\ \vdots & \vdots & \ddots & \vdots \\ r'(u_M)r(u_0) & r'(u_M)r(u_1) & \cdots & r'(u_M)r(u_M) \end{matrix} & \begin{matrix} B_{21} & & & B_{22} \end{matrix} \end{matrix} \tag{38}$$

Using the partition technique [13] to express $[R'R]^{-1}_{11}$ we have

$$(R'R)^{-1}_{11} = \xi^{-1}$$

where

$$\xi = r'(u_0)r(u_0) - B_{12}B_{22}^{-1}B_{21}$$

Substituting for B_{12} and B_{21} from (38) yields

$$\xi = r'(u_0)r(u_0) - [r'(u_0)r(u_1), \dots, r'(u_0)r(u_M)]B_{22}^{-1} \begin{bmatrix} r'(u_1)r(u_0) \\ \vdots \\ r'(u_M)r(u_0) \end{bmatrix} \tag{39}$$

The first term in (39) is easily evaluated

$$r'(u_0)r(u_0) = \eta^2(u_0)N \tag{40}$$

First notice that

$$B_{22}^{-1} = \begin{bmatrix} b_{22} & \cdots & b_{2M} \\ \vdots & & \vdots \\ b_{M2} & & b_{MM} \end{bmatrix}$$

where $b_{ts} = \beta_{st}/\det(B_{22})$ and β_{st} is the cofactor of the st element in B_{22} . In (39) expressions of the form $\mathbf{r}'(u_0)\mathbf{r}(u_t)\beta_{st}\mathbf{r}'(u_s)\mathbf{r}(u_0)$ are to be evaluated. For shorthand notation let $r_t \triangleq \mathbf{r}(u_t)$. β_{st} is a minor of $\det(B_{22})$ and, by definition, is the sum of all different signed products of the form $r'_1 r_{j_1}$, ..., $r'_M r_{j_M}$ excluding expression of the form $r'_s r_i$ and $r'_i r_t$ but including $r'_i r_s$ and $r'_t r_i$. The sequence j_1, j_2, \dots, j_M of second subscripts, is any one of the $M!$ permutations of the integers $1, 2, \dots, M$.

For example, the expression for $M=3; s=1, t=2$ is

$$q = r'_0 r_2 r'_2 r_1 r'_1 r_3 r'_3 r_1 r_0$$

and the explicit expression of q is

$$q = r'_0 \eta^2(u_2) \begin{bmatrix} 1 & e^{jk(a_1-a_2)u_2} & \cdots \\ e^{jk(a_2-a_1)u_2} & 1 & \cdots \\ \vdots & & \ddots \\ \vdots & & & 1 \end{bmatrix} \cdot \eta^2(u_3) N \eta^2(u_1) \begin{bmatrix} 1 & e^{jk(a_1-a_2)u_1} & \cdots \\ e^{jk(a_2-a_1)u_1} & 1 & \cdots \\ \vdots & & \ddots \\ \vdots & & & 1 \end{bmatrix}$$

Observe that the exponent is composed of a term which results from the elements of the diagonal adding up in phase and of a second term resulting from the summation of the randomly phased phasors. If the first term is assumed dominant, then q may be approximated by

$$q = \eta^2(u_0)\eta^2(u_1)\eta^2(u_2)\eta^2(u_3)N^2. \quad (41)$$

A similar result is obtained if $\eta^2(u_0)r'_1 r_2 r'_2 r_1 r'_3 r_3$, which corresponds to $\eta^2(u_2)r'_1 r_2 \beta_{12}$, is calculated. In the same fashion it can be shown that, in the general case, the following approximation holds

$$\mathbf{r}'(u_0)\mathbf{r}(u_t)\beta_{st}\mathbf{r}'(u_s)\mathbf{r}(u_0) \cong \eta^2(u_0)\mathbf{r}'(u_s)\mathbf{r}(u_t)\beta_{st}. \quad (42)$$

Returning now and developing the second term in (39) we write

$$B_{12}B_{22}^{-1}B_{21} = \frac{1}{|B_{22}|} (\mathbf{r}'(u_0)\mathbf{r}(u_1) \cdots \mathbf{r}'(u_0)\mathbf{r}(u_M)) \cdot \begin{bmatrix} \beta_{11} & \cdots & \beta_{M1} \\ \vdots & & \vdots \\ \beta_{1M} & \cdots & \beta_{MM} \end{bmatrix} \cdot \begin{bmatrix} \mathbf{r}'(u_1)\mathbf{r}(u_0) \\ \vdots \\ \mathbf{r}'(u_M)\mathbf{r}(u_0) \end{bmatrix} \\ = \frac{1}{\det(B_{22})} [\mathbf{r}'(u_0)\mathbf{r}(u_1)\beta_{11}\mathbf{r}'(u_1)\mathbf{r}(u_0) + \cdots \\ + \mathbf{r}'(u_0)\mathbf{r}(u_M)\beta_{M1}\mathbf{r}'(u_1)\mathbf{r}(u_0)] + \cdots \\ + [\mathbf{r}'(u_0)\mathbf{r}(u_1)\beta_{1M}\mathbf{r}'(u_1)\mathbf{r}(u_0) + \cdots \\ + \mathbf{r}'(u_0)\mathbf{r}(u_M)\beta_{MM}\mathbf{r}'(u_M)\mathbf{r}(u_0) + \cdots]$$

Using (40) and (42) together with the fact that the determinant of a matrix is the sum of products obtained by multiplying each element of a row by its cofactor (i.e., $\det(B_{22}) = \mathbf{r}'(u_m)\mathbf{r}(u_1)\beta_{m1} + \cdots + \mathbf{r}'(u_m)\mathbf{r}(u_M)\beta_{mM}$), we conclude that

$$B_{12}B_{22}^{-1}B_{21} = [\eta^2(u_0)^2/\det(B_{22})] \cdot [\det(B_{22}) + \cdots \\ + \det(B_{22})] \quad M \text{ times} \\ = \eta^2(u_0)M. \quad (43)$$

Therefore, substituting in (39) we get

$$\xi = \eta^2(n_0)(N-M), \quad (44)$$

and

$$(R'R)^{-1}_{11} = 1/\xi = \frac{1}{\eta^2(u_0)(N-M)}. \quad (45)$$

Finally (13) is obtained substituting (44) in (37)

$$\|W\|^2 = \frac{\alpha^2 N^2}{\eta^2(n_0)(N-M)}. \quad (46)$$

The expression in (46) for $\|W\|^2$ is an approximation based on (40) and (42). It is possible to verify (46) by examples. The factor α resulting from the approximation is a constituent of vector \mathbf{c} . Using α , the linear system of equations (2) is solved to obtain \mathbf{W} with minimum norm (12). Ideally $\|W\|^2 = N$, but due to the approximations $\|W\|^2$ and N will be somewhat different. This difference measures the accuracy of (46). Let the error be defined as

$$\text{error} = |N - \|W\|^2|/N. \quad (47)$$

EXAMPLES

A. Array 20 Elements

Nulls were imposed in the pattern of the array represented by Fig. 3 at $u = 0.4$. The sidelobe level is about -12 dB. The error is 0.8 percent. If the nulls are forced on the peak sidelobe at $u = 0.36$, the error jumps to 25 percent, since sums of phasors e^{jkau} considered nondominant and neglected in (42) are significant (as revealed by the existence of the peak sidelobe). The higher the sidelobe, the larger the error in (47).

B. Array 100 Elements

The array is represented by Fig. 9. Nulls were forced in a region of relatively high sidelobes, $u = 0.1$ (looking for the worst case). The error is 0.9 percent. No higher errors are expected.

It can be concluded in this Appendix that (46) describes $\|W\|^2$ with an error that is negligible for most of practical cases ($N > 100$).

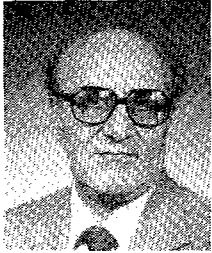
REFERENCES

- [1] C. L. Dolph, "A current distribution for broadside arrays which optimize the relationship between beam width and side lobe level," *Proc. IRE*, vol. 34, pp. 335-348, June 1946.
- [2] Ye. V. Baklanov, "A theory of linear antennas with unequal spacing," *Radio Eng. Electron. Phys.*, no. 6, pp. 905-913, June 1962.
- [3] D. S. Hicks and D. C. Patel, "Performance of thinned antenna arrays," presented at 1981 Int. IEEE Antennas Propagat. Symp., Los Angeles.
- [4] Y. T. Lo, "A mathematical theory of antenna array with randomly spaced elements," *IRE Trans. Antennas Propagat.*, vol. AP-12, pp. 257-268, May 1964.
- [5] B. D. Steinberg, *Microwave Imaging in Large Antenna Arrays*. New York: Wiley, 1983.
- [6] H. Steyskal, "Synthesis of antenna patterns with nulls," *IEEE Trans. Antennas Propagat.*, vol. AP-30, no. 2, pp. 273-279, Mar. 1982.
- [7] B. Steinberg, *Principles of Aperture and Array System Design*. New York: Wiley, 1976.

- [8] C. R. Rao, *Generalized Inverse of Matrices and its Applications*. New York, Wiley, 1971, pp. 44-46.
- [9] V. D. Agrawal and Y. T. Lo, "Distribution of side lobe level in random arrays," *Proc. IEEE*, vol. 57, pp. 1764-1765, Oct. 1969.
- [10] E. T. Whittaker, "On the functions which are represented by the expansion of the interpolation theory," *Proc. Roy. Soc. Edinburgh*, vol. 35, pp. 181-194, 1914-1915.
- [11] E. Isaacson, *Analysis of Numerical Methods*, New York: Wiley, 1966, p. 270.
- [12] R. Bellman, *Introduction to Matrix Analysis*. New York: McGraw-Hill, ch. 6, 7, 8.
- [13] J. Westlake, *A Handbook of Numerical Matrix Inversion*. New York: Wiley, 1968, p. 27.

Professor in Control and Communication Systems. During 1978/1979, he was on sabbatical with the Division of Applied Mathematics, Brown University. He was on leave of absence with the Department of System Engineering and the Valley Forge Research Center of the University of Pennsylvania and with Drexel University, Philadelphia. Currently, he is a member of the Technical Staff of AT&T Bell Laboratories, Holmdel, NJ. His interests include coherent communication, phase locked systems, signal processing, discrete control and adaptive systems and arrays.

Dr. Bar-Ness is a member of Sigma Xi and Eta Kappa Nu.



Yeheskel Bar-Ness (M'69-SM'78) was born in Iraq. He received the B.S. and M.Sc. in electrical engineering from the Technion, Israel, in 1958 and 1963, respectively, and the Ph.D. degree in applied mathematics from Brown University, Providence, RI, in 1969.

He worked for the Rafael Armament Development Authority, Israel, in the fields of communication and control, and as a Chief Engineer of the Nuclear Medicine Department, Elscint Ltd., Haifa, Israel, in the fields of control and image and data processing. In 1973, he joined the School of Engineering, Tel-Aviv University, Israel where he held the position of an Associate

neering, Tel-Aviv University, Israel where he held the position of an Associate



Alexander M. Haimovich (S'82-M'83) was born in Bucharest, Roumania, in 1954. He received the B.S. degree, cum laude, in 1977, from the Technion-Israel Institute of Technology, Haifa, Israel, and the M.S. in 1982, from Drexel University, Philadelphia, PA.

In the period of 1977-1982, he worked for the Israel Ministry of Defense. He is currently employed by American Electronic Laboratories, Inc., in the area of digital design.